Observing Forest Fires with the *GOES-8*, 3.9-μm Imaging Channel

JOHN F. WEAVER AND JAMES F. W. PURDOM

NOAA/NESDIS RAMM Branch, Colorado State University, Fort Collins, Colorado

TIMOTHY L. SCHNEIDER

Department of Atmospheric Science, Colorado State University, Fort Collins, Colorado

7 February 1995 and 15 June 1995

ABSTRACT

Blackbody radiation at 3.9 μm increases rapidly with temperature. This fact suggests a potential application by fire weather meteorologists of the 3.9-μm imagery data provided by the new *GOES-8* weather satellite. The ability of the 3.9-μm channel to sense forest fires is briefly discussed and an example case study is presented. A simple radiation model is used to estimate the minimum detectable fire size for several types of wildfires.

1. Introduction

Early and accurate detection is one of the most important aspects of forest fire management. Early detection alerts land management personnel (i.e., U.S. Forest Service, Bureau of Land Management, state or county personnel) to the existence of a fire in time to react quickly, while accurate locality information provides a basis for management decisions regarding an appropriate suppression response. Fires in overgrown wilderness regions may be allowed to burn—fires in regions having concentrations of people and/or structures may require an immediate and aggressive firefighting response.

Historically, the detection of forest fires has centered around reports from people; that is, from campers, hikers, rangers and lookouts at U.S. Forest Service observation towers. Today, as funding resources dwindle, remote sensors have increasing potential for augmenting these more traditional fire detection methods. Data from remote lightning detectors, or from Advanced Very High Resolution Radiometer (AVHRR) satellite imagery can greatly augment the human observer and help assure that expensive aircraft reconnaissance flights occur only when wild fires have actually been ignited. A comprehensive review of satellite-based fire-detection methodologies can be found in Chuvieco and Martin (1994a). Of course, fires may still go unreported for hours or even days. These unreported incidents may include, for example, 1) fires that ignite or begin spreading at night or in remote areas where human observers are typically not likely to spot the smoke, or 2) fires large enough to be detected on satellite, but that ignite between the currently available, twice-per-day AVHRR passes.

Recently, the National Oceanic and Atmospheric Administration (NOAA) has had placed in orbit a new Geostationary Operational Environmental Satellite, known as *GOES-8*, which is positioned approximately 22 245 miles (35 800 km) above the equator at a quasi-geostationary point. While the previous generation geostationary weather satellite has two dedicated imaging channels (visible and longwave infrared), *GOES-8* has five (see Menzel and Purdom 1994). These include the standard visible and long wave infrared channels, as well as a 6.7-μm channel (for upper-tropospheric moisture), a 12-μm channel (to help with the derivation of low-level moisture), and a shortwave infrared channel centered at 3.9 μm. Data from all five imaging channels will soon be routinely available for the entire hemisphere every 15 min. This new weather satellite may have utility within the fire management community, particularly at night, because certain attributes of radiation in the 3.9-μm range allow detection of active forest fires of only a few acres extent and these observations can be accessed with 15-min frequency.

2. The 3.9-μm response to subpixel hot spots

Matson and Dozier (1981) first addressed the sensitivity in the shorter wavelength infrared channels to subpixel hot spots. They proposed the simultaneous use of 3.7- and 11-μm data from NOAA polar-orbiting satellites for fire detection. Since then, radiation sensors on polar-orbiting satellites (such as the AVHRR) have been routinely used to monitor forest fires (e.g., Flannigan and Vonder Haar 1986; or Chuvieco and Martin

Corresponding author address: Dr. John F. Weaver, NOAA/NESDIS RAMM Branch, Colorado State University, Fort Collins, CO 80524.

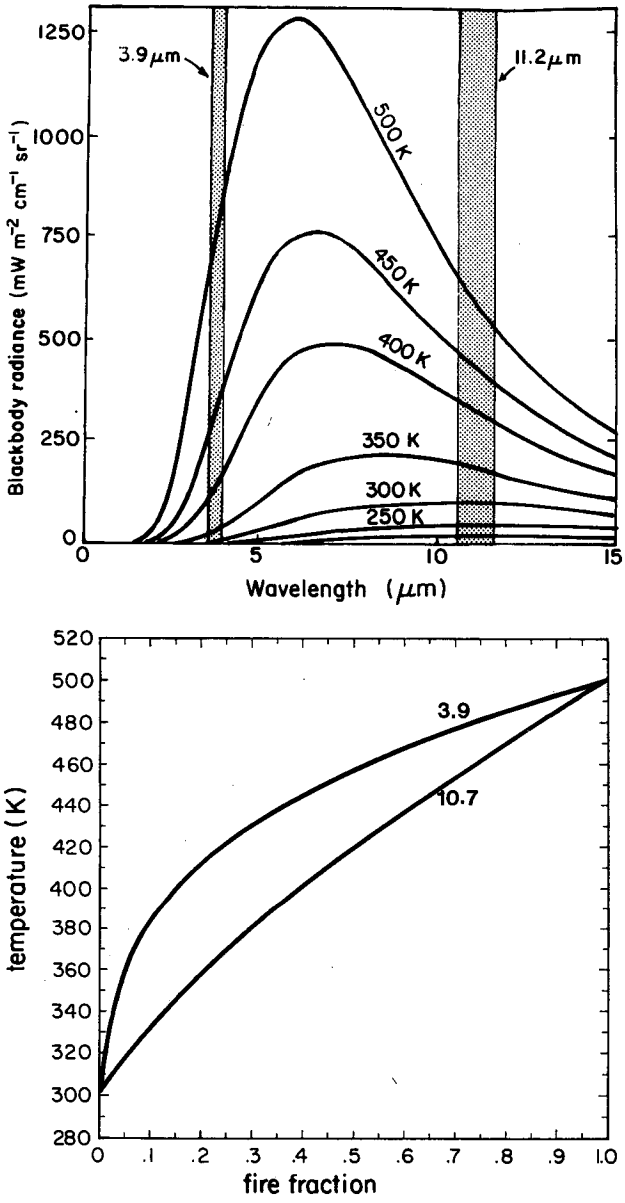

FIG. 1. (a) Plank radiances for temperatures from 200 to 500 K. The left shaded area is the response region for the 3.9-μm channel, the right shaded area is for 11.2 μm. The plot illustrates the relatively rapid response of the shorter wavelengths to heat (from Matson and Dozier 1981). (b) Graph showing brightness temperature in Kelvin (ordinate) versus fractional burning biomass (absissa) for both the 3.9- and 10.7-μm infrared channels on *GOES-8*. Data are computed assuming a 300 K background temperature and a 500 K temperature for the pixel fraction that is burning.

1994a,b). There have also been climatological studies of biomass burning in South America utilizing imaging and sounding channels on the previous GOES series satellites (Prins and Menzel 1994), though the spatial resolution on those instruments is poor.

The 3.9-μm channel is particularly useful in fire detection due, in part, to its dramatic response to subpixel hot spots. The charts shown in Fig. 1 illustrate the source and magnitude of this effect. Data for this example were computed assuming a 300 K background temperature and a temperature of 500 K for the burning region. Radiances are calculated for each area utilizing the Planck function,

$$B(\lambda, T) = \frac{C_1}{\lambda^5(e^{C_2/\lambda T} - 1)},$$

where B is the radiation emitted by a blackbody at wavelength λ for a surface at temperature T, and C_1, C_2, and c are universal constants. The resulting radiances are then weighted by the fraction of coverage at each temperature and summed. The final brightness temperatures are computed using the inverse of the Plank function.

As an example, note that if only 5% of a 2.3 km × 4.0 km picture element (the subpoint resolution of the *GOES-8* 3.9-μm channel) were burning at 500 K against a nonburning background temperature of 300 K, the brightness temperature of that element would rise from 300 K to around 360 K. These values, of course, ignore potential signal obscuration by smoke, overstory canopy, clouds, or blockage of the northern slopes of steep terrain due to viewing angle. Figure 1 also illustrates that this subpixel effect is far less noticeable in the longer wavelength IR data.

3. Detection example—The Pingree Park, Colorado, fire

a. Fire evolution

The main campus of Colorado State University (CSU) is situated in Larimer County, north-central Colorado, near the foothills of the Rocky Mountains in the town of Fort Collins. CSU also maintains a small subsidiary campus located in the mountains, 28 mi (45 km) due west of the main campus in a state-administered wilderness area known as Pingree Park. Prior to the forest fire of July 1994, the Pingree campus was composed of 57 buildings of varying size and usage including lecture halls, dining facilities, and lodging. The buildings were designed to provide a tranquil atmosphere conducive to scientific retreats—large, rustic-looking wooden structures built in the early 1900s, nestled in among mostly continuous stands of spruce, lodgepole pine, and aspen trees. Undergrowth in the region is composed of a variety of mixed-density Rocky Mountain vegetation and ground cover.

At approximately 0130 Local Standard Time (LST) 1 July 1994, a large thunderstorm moved across Larimer County. The storm produced little in the way of precipitation, but numerous lightning strikes were reported by visitors and residents in the Pingree Park region. Just after dawn, three small lightning-related fires were spotted by aircraft and subsequently extinguished. At 1030 LST, the fourth fire of the day was

reported about 1 mile west of the CSU facility. However, surface winds were light and variable, and the fire remained small throughout the remainder of the morning. Size estimates from Sheriff deputies on scene range from 5 to 10 acres (2 to 4 hectares). During this period, the fire was observed to creep slowly up the higher terrain to its west and south.

At about 1230 LST, the diurnal inversion mixed out and winds became westerly at 15–20 kt (8–10 m s^{-1}). The fire began to spread more rapidly. Within an hour it had moved into the canopies and began running eastward in the crowns. By 2100 LST that same evening, the fire had turned southeastward, slowed its forward progress, and was then burning more in the understory than in the crowns (although significant crown burning was still reported). By that time nearly 800 acres (160 hectares) had been scorched and two major spot fires were burning apart from the primary fire front (Fig. 2). The fire had traveled across the northwestern edge of the Pingree Park campus, totally destroying 12 structures and heavily damaging seven others.

b. GOES-8 observations and calculations.

Figure 3a shows the *GOES-8* 3.9-μm image from 2100 LST 1 July 1994. The three darker picture elements (pixels) are the ones being directly affected by the Pingree fire. Figure 3b shows the brightness temperature values in Kelvin associated with these pixels. Obscuration problems are thought to have been minimal. First of all, terrain in the region is not steep enough to block the view of any slopes. At 40°N, 105°W (the approximate coordinates of Pingree Park), the zenith angle of the *GOES-8* satellite is 41°, while slopes in the Pingree area are generally less than 10°. Also, at this time, the only clouds reported in the region were those from a scattered thin cirrus deck, so that cloud obscuration was not much of a problem. Just before sunset, smoke was observed to be advecting eastward. Since the satellite was viewing from nearly the due south, smoke obscuration was likely to have been minimal. Finally, since a significant part of the hottest burn was still in the crowns, and since the fire front was oriented orthogonal to the satellite viewing angle, overstory canopy effects were probably also very small. However, even should we assume that the combined effect of all four obscuration mechanisms taken together was nonnegligible, the implication would be *more* detection capability than that which will be estimated below, since we will be calculating minimum detectable sizes based upon the assumption that the Pingree region was completely unobscured.

The best-guess estimate of the nature and extent of the actual fire at this time will be compared, in a semi-rigorous fashion, to the 3.9-μm image. It is therefore important to document the source of the fire data. The geographical extent of the fire shown in Fig. 2 was supplied by the U.S. Forest Service, and by interviews with local firefighters who were on scene at the time. Temperature estimates were derived and fine-tuned through a series of roughly two dozen interviews with personnel from various emergency response agencies (see acknowledgments for list of participating interviewees). The temperature values presented are assumed to be accurate to within approximately 10% and correspond to median values measured by aircraft-mounted radiometers in a preliminary study of prescribed burns conducted in 1993.[1] This accuracy is more than sufficient for the illustrative nature of this note.

A few explanations of terminology are also in order. The *GOES-8* satellite scans the earth by sweeping 1-km swaths (i.e., 1-km high at the equator) alternately from east to west, then west to east, and so on, as it steps from the North Pole to south. The 3.9-μm sensor views an area which is 112 μrad × 112 μrad in size. This small area is called its *instantaneous field of view* (IFOV), and the scene is oversampled such that each final pixel is comprised of information from two IFOVs. Specifically, each final pixel is oversampled by a factor of 1.75. The actual area scanned at the ground varies. Directly beneath the satellite, the resolution of a single pixel is about 2.3 km × 4.0 km. We say that the resolution at *satellite subpoint* is 2.3 km × 4.0 km. Away from the satellite subpoint, a single pixel is larger due to increased viewing angles over the curved earth's surface. Thus, a single pixel is larger at higher latitudes and at increasingly different longitudes. For Pingree Park on this date, the individual pixel size was 3.1 km × 7.6 km. The reader may refer to Menzel and Purdom (1994) for a more detailed explanation of these and other aspects of *GOES-8* operations.

In order to relate the *GOES-8* scene to the actual fire, a few very general calculations will now be presented. The results are intended to help develop an understanding of how the GOES satellite interprets subpixel effects, rather than to precisely represent an actual retrieval. For the purposes of our simulations, we have subdivided the scene shown in Fig. 2 into a grid such that one IFOV is 150 × 93 subelements. The following assumptions have also been made.

- The scene is at night.
- All nonfire regions of the scene are at 286 K (the actual average observed temperature, at 3.9-μm wavelengths, of nearby pixels).
- The scene is *completely* unobscured.

---

[1] The experiment—known as Project Redsky—is a joint project between the Scitor Corporation, the Bureau of Land Management, the U.S. Forest Service, the U.S. Geological Survey (USGS), and the Department of Defense. Unpublished preliminary results from 1993 appear in an 11 page in-house memo entitled "Firefly Data from Sept. 28, 1993 Craig Colorado Fires" by Neil Hauser and Charles Snedaker. This document was made available to the authors by Neil Hauser (the Scitor Corporation, Aurora, CO) and Dr. Daryll G. Herd of the USGS.

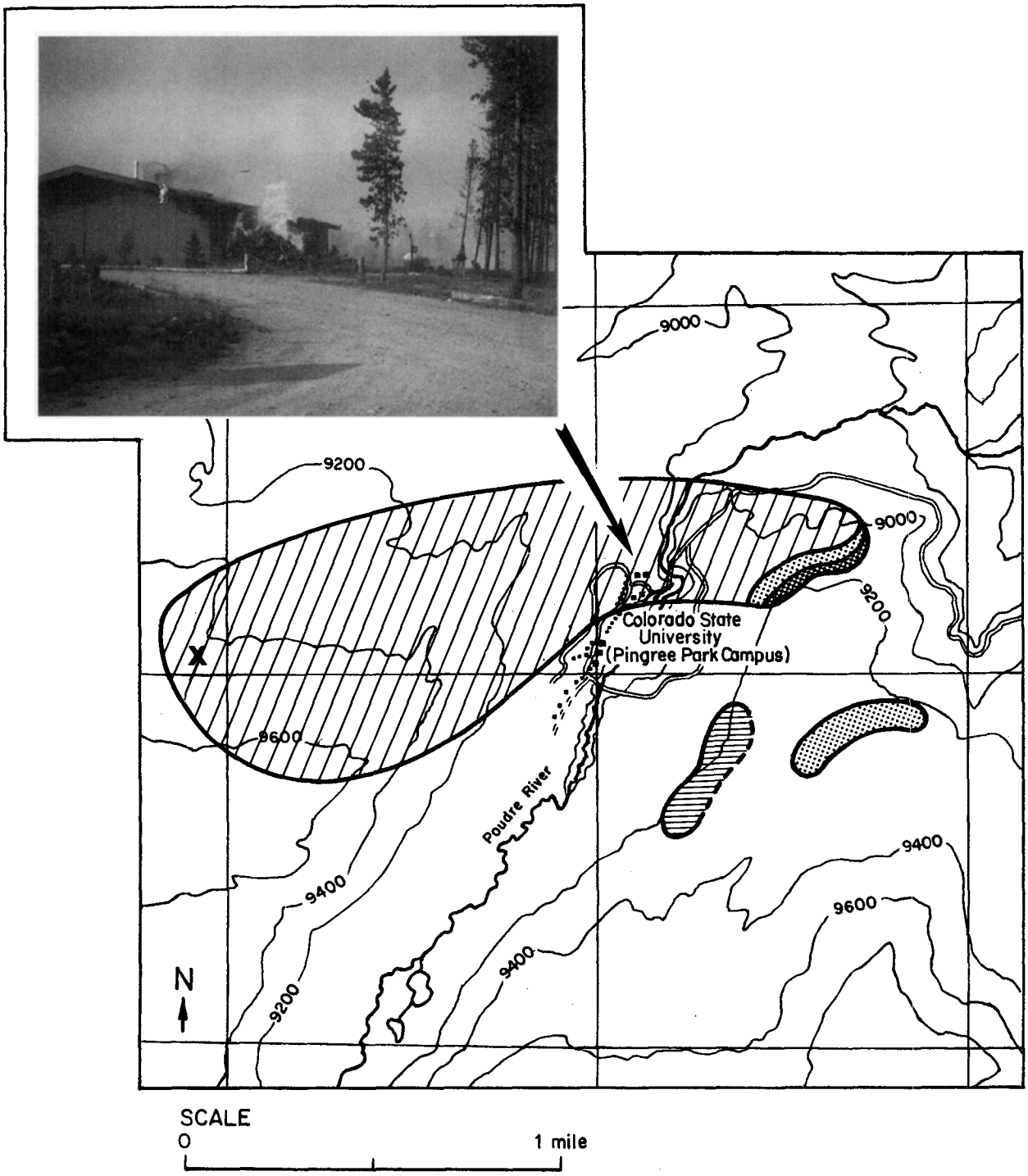

FIG. 2. Map of Pingree Park, Colorado, showing fire-affected areas as of 2100 LST 1 July 1994. The "X" indicates the fire's point of origin. The diagonally stripped, large region is a post-burn area that is smoldering at an assumed average temperature of 300 K; the horizontally stripped region is a spot fire burning at an assumed average temperature of 310 K; the light dotted regions are active surface burns at an assumed average temperature of 325 K; and the dark dotted region is the "fire front" burning at an assumed average temperature of 800 K. (*Inset: photo of the Pingree Park maintenance building shortly after a firebrand ignited a fire in a large wood pile stacked against the structure. This building was one of the seven that suffered heavy damage, but it was saved after firefighters threw the logs off to the side by hand. Photo courtesy of Ron Uthmann, Poudre Fire Authority, Ft. Collins, Colorado.*)

a

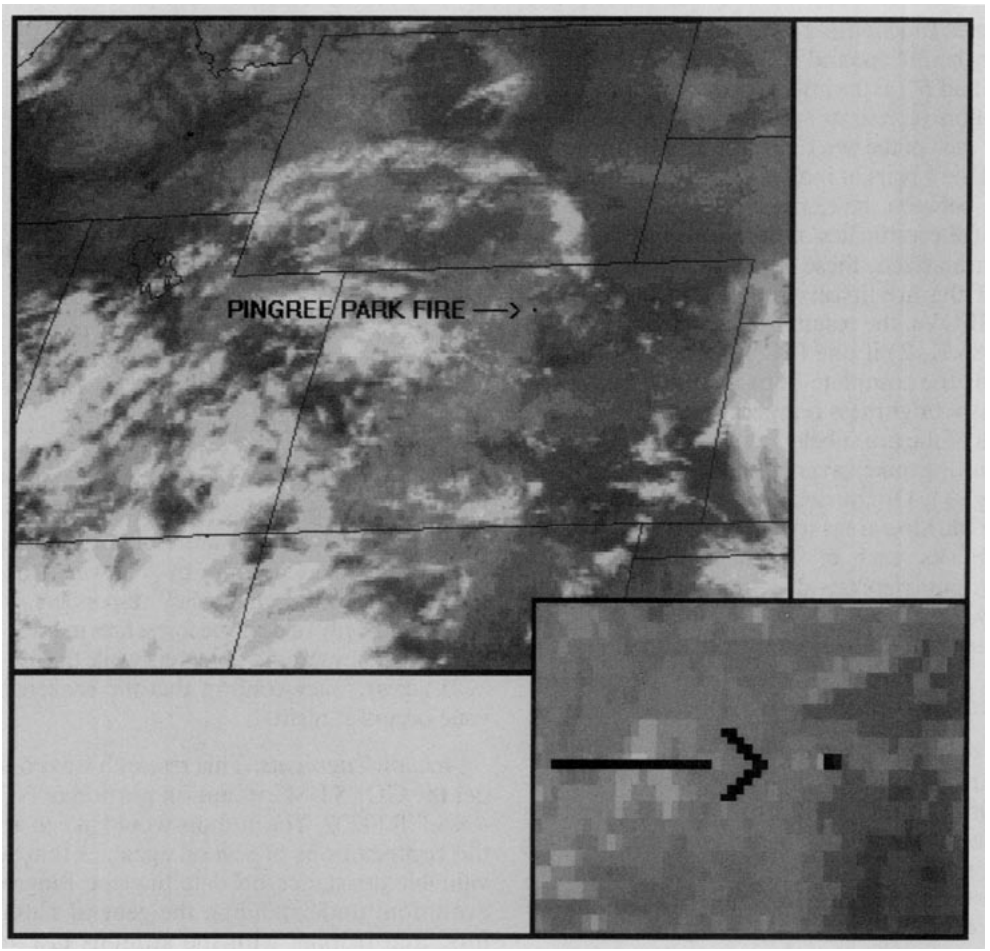

b

284.6	285.9	287.2	287.8	286.9
284.4	294.5	307.9	304.3	290.3
282.5	283.6	285.7	286.9	288.1

FIG. 3. *GOES-8* 3.9-μm image taken at approximately 2100 LST 1 July 1994. The figure shows (a) an overview of the image with a thumbnail inset of the local region, and (b) brightness temperatures in Kelvin for the fire-affected pixels and their immediate neighbors. An inverse color table, in which hotter pixels are darker, has been applied.

- All of the burning subelements fall within the IFOV with respect to the north–south direction (i.e., there are no hot pixels to the north or south of the affected pixels discussed in Fig. 3).
- Here, 3.9 μm is in a perfect atmospheric window (i.e., there is no atmospheric attenuation).
- Diffraction is negligible.
- There is no "lag" in sensor response.

These assumptions allow us to perform a simple average of the radiances for each subelement utilizing the Planck function. The averaging is carried out in radiance space due to the nonlinearity of the equation. Explicitly, the sensed effective brightness temperatures were computed using the following expression:

$$T_B = B^{-1}\left[\frac{1}{2N}\left(\sum_{i,j}\int_{\lambda_1}^{\lambda_2} B(\lambda, T_{i,j})d\lambda + \sum_{k,l}\int_{\lambda_1}^{\lambda_2} B(\lambda, T_{k,l})d\lambda\right)\right],$$

where the Planck function B is integrated from 3.8 to 4.0 μm (i.e., over the full spectral band of the *GOES-8*, 3.9-μm channel), and B^{-1} is the inverse of the Planck function. Each summation represents an average over all the subelements for each of the two IFOVs that make up a given pixel. The different pairs of indices (i, j and k, l) are used to distinguish between the respective IFOVs and are the two-dimensional coordinates of the gridded scene.

Briefly summarized, these computations show that 1) if none of the fire-involved, subelements fall into either of the IFOVs, the resultant pixel brightness temperature is 286 K, 2) if one IFOV is fire-free, and the other contains the complete burn area, the final averaged pixel has a brightness temperature of 299 K, and finally 3) if all of the fire subelements lie in both IFOVs, then the resulting pixel averages out to be 307.8 K (compare Fig. 3). Of course, there is a wide range of ways that the burning areas represented in Fig. 2 could fall within IFOVs, each of which would have to be considered in any rigorous development of a precise retrieval. However, those different contingencies do not affect the general interpretation presented below.

4. Final comments

The actual temperature values for the Pingree Park fire presented in this note are nothing more than rough estimates since fire temperature is a complex phenomenon depending upon a combination of fuel type, fuel moisture, density of combustibles, and atmospheric conditions. However, the temperatures values presented are realistic and it is completely accurate to say that, given a fire with the areal coverage and temperatures as estimated, the 3.9-μm channel on the *GOES-8* satellite would find pixel brightness temperatures similar to those actually observed.

Actually, much smaller fire areas are theoretically detectable under the conditions specified herein. If we apply the above method to estimate the minimum detectable fire size within an unobscured pixel, the results are quite interesting. Consider three types of burn areas as examples: 1) a wildfire burning at 325 K (e.g., a "typical" grass fire), 2) another at 450 K (e.g., a surface burn with heavy shrub that may be beginning to ladder into larger timber), and 3) a fire burning at 800 K (i.e., an active forest fire, beginning to move into the crowns). Also assume we are looking for pixels having temperatures at least 4 K above background, that is, a signal well above the sensor noise level of 1.5 K. The results shown in Table 1 indicate that unexpectedly small wildfires burning actively at these or similar temperatures would appear significantly warmer against the background temperature field of 286 K. Thus, fire weather meteorologists should be particularly interested in pixels that suddenly begin warming relative to their surroundings, particularly at night.

It should also be mentioned that while relatively small, hot fires are readily detectable by the 3.9-μm instrument, the 3.9-μm pixel saturates at 335 K. Anything hotter than that is off-scale. However, since the problem being addressed in this note is one of detection, this factor should have little, if any, effect. Also, whether saturated or not, hot pixels can also be used to monitor fire *growth* as discussed by Chuvieco and Martin (1994b).

TABLE 1. Detectable fire size versus subpixel burn temperature.

	325 K	450 K	800 K
All fire in one IFOV	1183 Acres	41 Acres	6 Acres
Fire in both IFOVs	592 Acres	21 Acres	2 Acres

As a final comment, it should be remembered that during daylight hours, the 3.9-μm signal is more difficult to interpret, because there is a strong reflected component to the radiation at this wavelength and because nonburning, neighboring pixels are warmer due to diurnal heating. However, during the day, 1-km visible data are available at 15-min intervals and fire weather meteorologists can confirm and track the fire by following smoke plumes. Furthermore, local emergency responders estimate that the vast majority of daytime forest fires in the United States are reported by ground observers while the fire is still small (1–5 acres). They confirm that the challenging spotting issue occurs at night.

Acknowledgments. This research was conducted under the GOES I-M evaluation portion of NOAA Grant #NA37RJ0202. The authors would like to acknowledge the contributions of several agencies that supplied invaluable assistance on detailing the Pingree Park fire evolution, understanding the general nature of forest fires, and helping with the arduous task of fire temperature estimation. Those involved include professionals from the U.S. Forest Service, Larimer County Emergency Services, Poudre Fire Authority, and the Fire Science Laboratory in Missoula, Montana. Special thanks are due Chuck Alluisi of the U.S. Forest Service and Dick Spiess of the Poudre Fire Authority for their careful reviews of the manuscript. We are also grateful to Dr. Phillip Gabriel for his expert help with some of the sensed-radiation calculations.

REFERENCES

Chuvieco, E., and M. P. Martin, 1994a: Global fire mapping and fire danger estimation using AVHRR images. *Photogramm. Eng. Remote Sens.*, **60,** 563–570.

——, and ——, 1994b: A simple method for fire growth mapping using AVHRR channel 3 data. *Int. J. Remote Sens.*, **15,** 3141–3146.

Flannigan, M. D., and T. H. Vonder Haar, 1986: Forest fire monitoring using NOAA satellite AVHRR. *Can. J. For. Res.*, **16,** 975–982.

Matson, M., and J. Dozier, 1981: Identification of subresolution high temperature sources using a thermal IR sensor. *Photogramm. Eng. Remote Sens.*, **47,** 1311–1318.

Menzel, W. P., and J. F. W. Purdom, 1994: Introducing GOES-I: The first of a new generation of geostationary operational environmental satellites. *Bull. Amer. Meteor. Soc.*, **75,** 757–781.

Prins, E. M., and W. P. Menzel, 1994: Trends in South America biomass burning detected with the GOES visible infrared spin scan radiometer atmospheric sounder from 1983 to 1991. *J. Geophys. Res.*, **99**(D8), 16 719–16 735.